

AperTO - Archivio Istituzionale Open Access dell'Università di Torino

**Spectroscopic characterization and photo/thermal resistance of a hybrid palygorskite/methyl red Mayan pigment**

**This is the author's manuscript**

*Original Citation:*

*Availability:*

This version is available <http://hdl.handle.net/2318/93773> since

*Published version:*

DOI:10.1016/j.micromeso.2012.01.024

*Terms of use:*

Open Access

Anyone can freely access the full text of works made available as "Open Access". Works made available under a Creative Commons license can be used according to the terms and conditions of said license. Use of all other works requires consent of the right holder (author or publisher) if not exempted from copyright protection by the applicable law.

(Article begins on next page)

This Accepted Author Manuscript (AAM) is copyrighted and published by Elsevier. It is posted here by agreement between Elsevier and the University of Turin. Changes resulting from the publishing process - such as editing, corrections, structural formatting, and other quality control mechanisms - may not be reflected in this version of the text. The definitive version of the text was subsequently published in MICROPOROUS AND MESOPOROUS MATERIALS, 155, 2012, 10.1016/j.micromeso.2012.01.024.

You may download, copy and otherwise use the AAM for non-commercial purposes provided that your license is limited by the following restrictions:

- (1) You may use this AAM for non-commercial purposes only under the terms of the CC-BY-NC-ND license.
- (2) The integrity of the work and identification of the author, copyright owner, and publisher must be preserved in any copy.
- (3) You must attribute this AAM in the following format: Creative Commons BY-NC-ND license (<http://creativecommons.org/licenses/by-nc-nd/4.0/deed.en>), 10.1016/j.micromeso.2012.01.024

The publisher's version is available at:

<http://linkinghub.elsevier.com/retrieve/pii/S1387181112000340>

When citing, please refer to the published version.

Link to this full text:

<http://hdl.handle.net/2318/93773>

# Spectroscopic characterization and photo/thermal resistance of a hybrid palygorskite/methyl red Mayan pigment

Roberto Giustetto<sup>\*1,2</sup>, Kalaivani Seenivasan<sup>2,3</sup>, Diego Pellerej<sup>2,3</sup>, Gabriele Ricchiardi<sup>2,3</sup>, Silvia Bordiga<sup>2,3</sup>

<sup>1</sup> Department of Earth Sciences,  
Università di Torino, Via Valperga Caluso 35, 10125 Torino, Italy

<sup>2</sup>NIS Centre of Excellence, via Quarelo 11, 10135 Torino, Italy

<sup>3</sup> Department of Inorganic, Physical and Materials Chemistry, INSTM Centro di Riferimento,  
Università di Torino, Via P. Giuria 7, 10125 Torino, Italy

\*Corresponding author tel. no.: +390116705122; e-mail: roberto.giustetto@unito.it

## Abstract

The structural features and host-guest interactions existing in a stable, red-purplish hybrid material obtained by grinding and heating palygorskite clay with 2 wt% acid Red 2 (methyl red) were investigated by means of vibrational and UV-vis spectroscopies in controlled experimental conditions and TGA analyses. Experimental evidences suggest that modified methyl red molecules, in the form of specific zwitterions and/or altered trans-isomers, can diffuse inside the palygorskite tunnels or superficial grooves once zeolitic H<sub>2</sub>O is removed due to heating or vacuum. The dye is likely to interact with the palygorskite framework by means of several bond types, which include H-bonding to Mg-coordinated OH<sub>2</sub> and electrostatic forces, responsible for the compound stability. Sorption in the hosting matrix enhances both the photo- and thermal stability of methyl red and increases steadiness of the palygorskite structure by preventing folding with progressive heating. Such a hybrid material, which shows the same stability and structural features of the famed *Maya Blue* used in Pre-Columbian America, could therefore be used as an innovative *Maya Red* pigment.

**Keywords:** palygorskite; acid Red 2 (methyl red); Maya Blue; dye encapsulation; dye stabilization.

## 1. Introduction

Modern host/guest hybrid materials are of fundamental importance nowadays for their various and multipurpose applications. Inclusion compounds obtained by sorption of cations and/or small molecules in meso- and microporous materials can be employed in a wide range of specific fields, such as optical carriers, polymer reinforcement, and photonic antennas.<sup>1-4</sup> In addition, similar host/guest adducts can find more immediate applications as polymer reinforcement, paints and pigments.<sup>5</sup> Zeolitic aluminosilicates are valid and versatile hosting materials for the supramolecular organization of a wide variety of possible guests<sup>6</sup> due to both their activity and presence of structural cavities, but other microporous silicates can be used as well.

Palygorskite and sepiolite are phyllosilicate microporous clay minerals renowned for their ability to trap ionic species (such as  $Mn^{2+}$  and  $Pb^{2+}$ )<sup>7,8</sup> and/or little molecules (i.e. polypropylene and ammonia or sulphur dioxide).<sup>9,10</sup> In addition, both clays – but especially the former – are important in Cultural Heritage being the inorganic matrices of a famous ancient Pre-Columbian pigment: Maya Blue. Such a compound can be considered an ancestor of modern hybrid materials, for an organic guest molecule (indigo, a well-known blue dye) is adsorbed within the micropores of the hosting palygorskite and/or sepiolite frameworks. This pigment was mainly produced by the ancient Mayas in the Yucatán Peninsula (Mexico) from VII to XVI century a.D. and used to decorate mural paintings, statues and pottery. It is renowned for its exceptional chemical stability to both acid and alkali reagents. Though the historical sources describing the ancient pigment preparation are few and incomplete,<sup>11</sup> a general agreement exists about the synthesis procedure of freshly-prepared Maya Blue analogues – both using raw methods (clay extracted from local outcrops and indigo from the leaves of *Indigofera Suffruticosa* tree)<sup>11</sup> or pristine precursors.<sup>12,13</sup> Such a procedure requires palygorskite clay to be ground with indigo ( $\leq 2$  wt%) and moderately heated ( $< 200^{\circ}C$ ) for a variable amount of time (30 minutes to few hours). Heating is fundamental as a barely ground palygorskite/indigo mixture, though similar in aspect to Maya Blue, is completely discolored by acid attack.

The structure of palygorskite [ideal formula:  $(\text{Mg},\text{Al})_4\text{Si}_8\text{O}_{20}(\text{OH})_2(\text{OH}_2)_4 \cdot 4\text{H}_2\text{O}$ ] is based on a continuous, waving tetrahedral sheet in which the  $\text{SiO}_4$  tetrahedrons periodically (every two pyroxene-like chains) invert the orientation of their apical oxygens, which are bonded to  $z$ -elongated, discontinuous octahedral ribbons containing both Mg and Al ions (Fig. 1.a).<sup>14</sup> Such an arrangement causes the structure to be crossed by microtunnels ( $6.4 \times 3.7 \text{ \AA}$ ), elongated in the  $z$ -axis direction, usually filled by weakly-bound zeolitic  $\text{H}_2\text{O}$  molecules interconnected through a complicated web of H-bonds.<sup>15</sup> Tightly-bound structural water ( $\text{OH}_2$  in the following)<sup>16</sup> is coordinated by Mg ions located in the  $M3$  sites on the edges of the octahedral strips.<sup>17,18</sup>

(INSERT FIGURE 1)

Indigo in Maya Blue is expected to diffuse, although at a limited extent, inside the palygorskite tunnels partially emptied from zeolitic  $\text{H}_2\text{O}$  during heating<sup>19-22</sup> and form specific host/guest interactions with the clay matrix, whose nature is still disputed.<sup>23-33</sup> The amount of indigo binding to the clay, though dependent from the magnitude of the applied heating, is reputed to be quite low ( $\leq 2 \text{ wt\%}$ ).<sup>13,19-21,25</sup> Encapsulation and bonding within the clay tunnels shield the dye molecules from external environment thus ensuring the pigment stability to chemical agents. Basing on such premises, the extraordinary sorption properties of palygorskite were exploited to stabilize differently coloured dye molecules with the aim to synthesize innovative hybrid materials useable as pigments in the Cultural Heritage, Materials Science and paint industry fields. Such an approach, seldom adopted in the past to remove dyes from wastewater solutions<sup>34,35</sup> or evaluate the stability of analogous clay/dye adducts,<sup>23,27,28</sup> could lead to production of compounds granted by limited toxicity (absence of heavy-metals, poisonous for human health) and low production expenses. In a previous paper Giustetto and Wahyudi<sup>36</sup> succeeded in synthesizing a stable red-purple hybrid pigment by grinding and heating palygorskite with 2 wt% acid red 2 ( $\text{C}_{15}\text{H}_{15}\text{N}_3\text{O}_2$ , C.I. 13020 – Fig.1.b; methyl red hereafter), an azo-dye used as pH indicator (red at  $\text{pH} \leq 4.4$ ; yellow at  $\text{pH} \geq 6.2$ ; orange in between). Fixation of methyl red in palygorskite stabilizes the dye molecule preventing colour changes in spite of

severe pH fluctuations. Such a compound proved to possess a chemical stability comparable to Maya Blue as both its hue and structure are virtually unaltered after attacks with acid and alkali solutions (modified version of the Gettens test).<sup>37</sup>

Picking up the baton from these evidences, the current paper deals with the further in-deep characterization of both the structure and the nature of the host-guest interactions responsible for stabilization of this palygorskite + methyl red (2 wt%) adduct. Though fixation of methyl red was tentatively experimented on laminar clays (i.e. montmorillonite and vermiculite),<sup>38</sup> zeolites<sup>39</sup> and Ni-Fe layered materials,<sup>40</sup> this never attempted before adsorption on palygorskite brings to formation of an innovative hybrid material which, due to its composition and colour, could rightfully be considered a modern, organic-inorganic hybrid *Maya Red* pigment.

## 2. Experimental

### 2.1 Synthesis

Natural palygorskite, coming from Chapas (Mexico), was hand-ground and purified through dispersion into de-ionized water isolating the thinner suspended fraction from the heavier quartz and calcite impurities.<sup>15</sup> X-ray powder diffraction data, collected on an automated Siemens D-5000 diffractometer in Bragg-Brentano geometry using graphite monochromatized  $\text{CuK}_\alpha$  radiation and a zero-background flat sample holder, proved palygorskite to be the only detectable phase. Solid acid red 2 (methyl red) powder [4-( $\text{CH}_3$ )<sub>2</sub>NC<sub>6</sub>H<sub>4</sub>N:NC<sub>6</sub>H<sub>4</sub>·2-COOH] was provided by Carlo Erba (C.I. 13020).

Procedure for the synthesis of the palygorskite + methyl red (2 wt%) adduct was exhaustively described in a previous paper<sup>36</sup> and modeled upon the laboratory preparation of Maya Blue from pure precursors.<sup>12,13,23,41</sup> Crushed palygorskite was mixed and hand-ground with 2 weight% of methyl red powder (consistently with the maximum indigo amount in Maya Blue)<sup>13,19,20,21,25</sup> adding few drops of ethanol. The so-obtained orange mixture, which

turned to brilliant red after a few minutes, was dispersed in a Petri dish with diluted HCl (20%) and heated from room temperature up to 140°C through progressive 20°C/hour increase steps; global heating time was 20 hours. The resulting red-purplish compound was Soxhlet-extracted in ethanol to remove dye-surplus, turning to a bright purple-violet hue. A different procedure was adopted to synthesize the specimens studied by infrared (IR) spectroscopy. Palygorskite was preliminarily activated in vacuum (pressure below  $5 \times 10^{-4}$  mbar in N<sub>2</sub> atmosphere) at 120°C for 2 hours in order to remove zeolitic H<sub>2</sub>O and then ground with 2 wt% methyl red (activated at 120°C for 30 minutes) in glove-box under N<sub>2</sub> atmosphere. The resulting mixture was pressed in a pellet and inserted in a IR cell inside the glove box. After N<sub>2</sub> removal, the specimen was further heated in vacuum at 150°C. IR absorption spectra were collected in each synthesis step (before and after heating).

## *2.2 Methods*

IR absorption spectra were collected under controlled atmosphere (N<sub>2</sub>) and/or in vacuum (pressure below  $5 \times 10^{-4}$  mbar) on a FTIR Bruker Vector 70, with a resolution of 2 cm<sup>-1</sup> and collecting 64 scans for each spectrum.

Raman data were collected using several Renishaw in Via- or micro-Raman Microscopes equipped with diode (emitting at 785 nm), He-Cd (325 nm) or Ar<sup>+</sup> lasers (514 and 244 nm). Scattered photons were dispersed by a 1800 or 3600 lines/mm grating monochromator respectively and collected on CCD cameras. The collection optic was set at 15 or 20X objectives respectively.

UV-visible-NIR spectra in diffuse reflectance mode were collected using a Varian Cary 5000 spectrophotometer in the 2500-200 nm range on samples previously diluted with BaSO<sub>4</sub> (1:3/1:20).

Photo-stability was tested through progressively increasing irradiation times under a Solarbox CoFoMegra 3000i, providing a solar like spectrum (250 W/m<sup>2</sup>, 40°C irradiation chamber) and under an Osram Ultra Vitalux 300W mercury vapour lamp, providing a UV-A spectrum (40 W/m<sup>2</sup>, 60°C). Irradiation was performed on BaSO<sub>4</sub> diluted (1:3) specimens, crushed in an agate mortar and finely dispersed on clock glasses in order to maximize exposure and avoid possible measure-altering covering. At prefixed times, the irradiated powders were transferred and pressed in an Al sample-holder with a suprasil quartz window and their optical features analyzed by means of diffuse reflectance UV-Vis spectroscopy. After data collection, specimens were re-crushed and dispersed for further irradiation. Thermogravimetric data were collected on a Diamond TG/DTA instrument (Perkin Elmer) in air and N<sub>2</sub> flux, 40°C equilibration with a heating rate of 20°C/min until 1000°C temperature was reached. Stability to thermal treatment was also checked by evaluation of the hybrid material optical features by means of diffuse reflectance UV-Vis spectroscopy, collecting spectra on specimens in the form of finely dispersed BaSO<sub>4</sub> diluted (1:3) powder films progressively heated in oven for 2 hours periods at pre-fixed increasing temperatures.

### 3. Results

#### *3.1 Spectroscopic characterization*

Spectroscopic data on the palygorskite + methyl red (2 wt%) adduct were collected on both isolated precursors and on the resulting hybrid material in all different steps of the synthesis procedure. Several attempts were made at collecting Raman spectra, but strong fluorescence effects related to both the dye<sup>42-46</sup> and the clay matrix<sup>25,47-49</sup> made it impossible to obtain acceptable data.

(INSERT FIGURE 2)



Fourier Transform Infra-red (FTIR) spectra for the palygorskite + methyl red (2 wt%) adduct collected in average environmental condition (in air at room temperature)<sup>36</sup> hinted the feasible existence of host/guest interactions between the clay and the dye, though nothing could be stated about their nature nor the reactive groups possibly involved in their formation. This information, in fact, is hidden under the broad and intense signals related to presence of physisorbed water on the clay fibres surface and zeolitic H<sub>2</sub>O in the tunnels, which may cover other important IR-active modes related to both the clay and the dye. To overcome this problem and grab information about the establishment and nature of mutual bonds during the pigment preparation, an innovative approach successfully adopted in previous studies on analogous clay/dye adducts<sup>25,41,50</sup> was followed. The evolution of the IR-spectra was monitored on a pre-activated palygorskite specimen mixed and ground in controlled atmosphere with pre-activated methyl red (2 wt%), both before and after heating in vacuum (pressure below  $5 \times 10^{-4}$  mbar in N<sub>2</sub> atmosphere). These FTIR evidences, purged of the troublesome effects related to presence of weakly-bound H<sub>2</sub>O, were compared to those collected in average environmental conditions and to previous results obtained with other techniques (i.e. UV-vis spectroscopy).<sup>36</sup>

FTIR data collected on the clay/dye adduct in separate synthesis steps under controlled experimental conditions are summarized in Figure 2, part (b) and compared with the spectra of pristine solid-state methyl red dispersed in KBr or solvated in benzene [Figure 2, part (a), grey and black patterns respectively]. The most relevant IR-active bands of methyl red appear in the 1800-1100 cm<sup>-1</sup> interval [although weak signals, due to  $\nu(\text{C-H})$  of aromatic and aliphatic groups, appear between 3800 and 2800 cm<sup>-1</sup>]. Moving from higher towards lower frequencies, main components can be observed at: i) 1712 cm<sup>-1</sup>, related to the stretching of the carbonyl group [ $\nu(\text{C=O})$ ]; ii) 1601 and 1367 cm<sup>-1</sup>, due to  $\nu_{\text{asym}}(\text{N=N})$  and  $\nu_{\text{sym}}(\text{N=N})$  bonds typical of azo dyes;<sup>40,51</sup> iii) doublet at 1364 and 1340 cm<sup>-1</sup>, due to  $\nu(\text{C-}$

C); iv) 1483  $\text{cm}^{-1}$ , associated with  $\tau(\text{C-N})$ ; v) 1312 and 1277  $\text{cm}^{-1}$ , assigned to mixed modes with  $\nu(\text{C-C})$ ,  $\delta(\text{C-H})$ ,  $\delta(\text{C-N})$ <sup>51</sup> or with  $\delta(\text{N-H})$  and  $\nu(\text{N-ring})$ <sup>52</sup> characters; vi) 1269  $\text{cm}^{-1}$ , due to  $\delta(\text{O-H})$ ; vii) 1146  $\text{cm}^{-1}$ , associated to  $\nu(\text{C-O})$ . Most of these bands appear narrower passing from the solid-state KBr-diluted dye [grey curve in Fig. 2, part (a)] to the benzene-dissolved specimen [black curve in Fig. 2, part (a)]; in addition, the  $\nu(\text{C=O})$  signal shifts to higher frequency (1742  $\text{cm}^{-1}$ ).

The FTIR spectrum of a thin palygorskite film deposited on a silicon wafer at different hydration levels was described by Giustetto et al..<sup>25</sup> Palygorskite in air show bands due to zeolitic  $\text{H}_2\text{O}$  and structural  $\text{OH}_2$  both in the stretching (3800-2800  $\text{cm}^{-1}$ ) and in the bending regions (1750-1600  $\text{cm}^{-1}$ ). By evacuating the clay, components related to weakly bound  $\text{H}_2\text{O}$  progressively disappear as sharper bands related to structural  $\text{OH}_2$  and framework OH (only hydrated and hydroxyl components known to exist in evacuated palygorskite)<sup>53,54</sup> emerge. Further heating implies shifting of the IR-active modes due to gradual  $\text{OH}_2$  loss (expected to start at 80°C in vacuum)<sup>55</sup> and consequent structure folding. Once temperature reaches 150°C in vacuum three main bands appear, assigned to the stretching of framework hydroxyls (3644  $\text{cm}^{-1}$ ) and coordinated  $\text{OH}_2$  (3582 and 3525  $\text{cm}^{-1}$ ) respectively,<sup>25</sup> all perturbed due to folding of the clay structure as a result of approximately 50%  $\text{OH}_2$  loss. Such a loss can be directly quantified from the decay in intensity of the  $\text{OH}_2$  bending mode at 1620  $\text{cm}^{-1}$ .<sup>55-58</sup> The spectral trend observed in the current study is consistent with the above described situation, though a sharp distinction of all mentioned IR maxima could not be achieved due to measurements being performed on a pellet instead of a thin film. Further heating (> 600°C) implies disappearance of these bands due to irreversible  $\text{OH}_2$  loss and transformation to palygorskite-anhydride (spectra not shown).

When 2 wt% activated methyl red is mixed and ground in controlled  $\text{N}_2$  atmosphere with an evacuated/pre-activated palygorskite specimen, the IR spectrum shows the simultaneous

presence of vibrational modes related to both the clay and the dye [Fig. 2, part (b), curve 1]). Most significant methyl red modes can be observed in the 1250-1550  $\text{cm}^{-1}$  interval, where no superposition with the more intense clay features occurs. Principal variations affecting the signals of clay-solvated methyl red with respect to those of the isolated dye can be summarized as follows: i) maxima at 1277 and 1312  $\text{cm}^{-1}$ , evident in pure methyl red [Fig. 2, part (a)], undergo a significant intensity decrease when the dye is ground with the activated clay, becoming barely visible; the band at 1398  $\text{cm}^{-1}$  [ $\nu(\text{N}=\text{N})$ ], conversely, shows an opposite intensity increase [Fig. 2, part (b), curve 1]. Similar behaviors were also observed for methyl red ground and heated in air with non pre-activated palygorskite<sup>36</sup> or intercalated in different matrices<sup>40</sup> and suggest possible existence of supramolecular host/guest interactions. ii) both the intensity increase of the 1398  $\text{cm}^{-1}$  maximum and the shift at lower frequencies (from 1483 – pristine dye – to 1502  $\text{cm}^{-1}$  – clay/dye adduct) of the  $\tau(\text{C}-\text{N})$  band suggest possible transformation of methyl red to one of its quinoid zwitterionic intermediates, an occurrence already observed in literature.<sup>36</sup> iii) maximum at 1742  $\text{cm}^{-1}$  [ $\nu(\text{C}=\text{O})$ ]<sup>40</sup> undergoes a significant red-shift peaking at 1690  $\text{cm}^{-1}$  [Fig. 2, part (b), curve 1], implying possible carbonyl perturbation due to H-bond formation.

As far as the palygorskite modes are concerned, lack of decay in the bending mode of Mg-coordinated  $\text{OH}_2$  (1620  $\text{cm}^{-1}$ ) certifies that the applied evacuation caused no structural  $\text{OH}_2$  loss.<sup>53,54</sup> Magnification on this band high-frequency side (Fig. 2, inset c) shows the appearance of a tiny shoulder at higher wavenumbers (1632  $\text{cm}^{-1}$ ), claiming perturbation of a small  $\text{OH}_2$  fraction possibly involved in the formation of H-bonds.<sup>25-41-50</sup> In the hydroxyls stretching region, being the undiluted clay/dye specimen a pellet instead of a thin film, the most intense components go out of scale in the range 3650-3515  $\text{cm}^{-1}$  thus hiding the contributions of framework OH and coordinated  $\text{OH}_2$  [3644 and 3525  $\text{cm}^{-1}$  respectively].<sup>54,55</sup> On the high frequency side of the main absorption, however, a weak doublet [3690 and 3714

$\text{cm}^{-1}$  – Fig. 2, part (b), curve 1] can be related to  $\text{OH}_2$  interacting with the non-polar part of the azo dye. Furthermore, appearance of a shoulder on the low frequency side at  $3372 \text{ cm}^{-1}$  can be related to a small  $\text{OH}_2$  fraction being perturbed (and red-shifted) due to H-bond formation; such a signal may therefore represent the counterpart in the stretching region of the analogous weak signal ( $1632 \text{ cm}^{-1}$ ) in the bending interval, a correspondence already signaled in similar sepiolite-based adducts with indigo.<sup>41,50</sup>

When the ground palygorskite + methyl red (2 wt%) adduct is further heated [ $150^\circ\text{C}$  in vacuum – Fig. 2, part (b), curve 2], no significant variations other than slight intensity differences apparently affect the IR spectrum. No major intensity decrease is observed for the  $\delta(\text{OH})$  mode of coordinated  $\text{OH}_2$  ( $1620 \text{ cm}^{-1}$ ), implying that in spite of the applied heating loss of structural  $\text{OH}_2$ , if any, is scarce. Furthermore, only minor changes affect the OH stretching region; persistence of strong absorptions in the  $3650\text{-}3515 \text{ cm}^{-1}$  range and of the doublet at  $3690$  and  $3714 \text{ cm}^{-1}$  [Fig. 2, part (b), curve 2] indicate an approaching of methyl red reactive groups ( $\text{CH}_3$  or phenyl) to the hexagonal hole of the amphibole-like tetrahedrons chain, possibly due to dye encapsulation. Little can be said unfortunately on the coordinated  $\text{OH}_2$  modes which possibly play a fundamental role in the establishment of the stabilizing host/guest interactions, as the related bands go out of scale.

Further rehydration and Soxhlet extraction in ethanol [Fig. 2, part (b), curve 3] cause, as expected, broadening and shifting of the clay-related  $\delta(\text{OH})$  IR maximum (peaking now at  $1648 \text{ cm}^{-1}$ ) and significant intensity decrease of all dye-related features, due to zeolitic  $\text{H}_2\text{O}$  re-absorption and excess methyl red being washed out respectively.

### *3.2 Resistance to solar/UV-A irradiation and thermal treatment*

In order to further characterize the stability of the studied hybrid material, resistance to different kinds of irradiation and heating were tested and compared to those shown by the

isolated precursors. Such features were evaluated by comparing the optical properties of the material before and after exposure.

### *3.2.1 Photo-stability*

The photo-stability of a heated and Soxhlet-extracted palygorskite + methyl red (2 wt%) specimen was tested through prolonged exposure under solar and UV-A irradiation. Fig. 3.a shows the diffuse reflectance UV-vis spectra collected at progressively increasing times (up to 100 hours) under a solar-like irradiation. It is evident how the absorption maxima, both in the visible (540 and 580 nm) and in the UV (245 nm) regions, show marked intensity decrease in time as a result of a progressive bleaching of the material. Such a fall follows different trends for the two visible maxima, as the 580 nm band undergoes a less marked decay than its 540 nm counterpart (40% vs. 45% after 100 hours, reaching 60% and 55% of their original heights respectively: Fig. 3.b). At the end of the exposure, the mutual intensities of the two maxima become reversed (Fig. 3.a).

For comparison purposes, pristine methyl red powders were irradiated under the same conditions. The related diffuse reflectance UV-vis spectra collected at pre-fixed intervals (not shown) prove that an analogous intensity decrease affects in equal measure all three main absorption bands (290, 465 and 575 nm respectively) due to progressive dye degradation. This fall in intensity is sensibly quickened in time with respect to that observed for the clay-adsorbed dye. Stability to solar irradiation is therefore vigorously enhanced by fixation of methyl red in the microporous matrix.

(INSERT FIGURE 3)

The effect of prolonged UV-A irradiation (up to 76 hours) on the spectral features of the studied hybrid material is shown in Fig. 4. Absorption maxima in the visible region

(540 and 580 nm) show a progressive intensity decay in time, symptomatic of an intervened dye degradation. Both bands are affected in equal measure, so that the ratio of their mutual intensities remains unvaried.

The global intensity decay and bleaching of the studied compound is slightly more enhanced than that observed under a solar-like irradiation, even if measured on shorter exposure times (42% intensity decrease for the 580 nm peak after 76 hrs: Fig. 4.b), which is consistent with the higher energy emitted by the UV-A irradiating lamp. No significant shift affects the positions of the absorption maxima throughout all exposure, though the two bands tend to gradually coalesce in a single broad feature. Such a trend suggests that no transformation affects the dye molecules but rather a gradual decay and consequent bleaching.

Interpretation of diffuse reflectance UV-vis spectra collected on pure methyl red exposed to the same UV-A irradiation (not shown) is troublesome, as the intensity variations of the absorption bands are not linearly related to different exposure times.

(INSERT FIGURE 4)

### 3.2.2 *Thermal stability*

Thermograms (TGA) and Heat Flow (DSC) data were collected for pure palygorskite, methyl red and for the studied red-purplish hybrid material. Patterns were collected both in air and N<sub>2</sub> flux, but no appreciable difference was observed. The following comments and related figures are referred to data collected in air.

The TGA/derivative Heat Flow (DSC) patterns for pure palygorskite (Fig. 5) are consistent with previous studies<sup>15,59-61</sup> and can be divided in three sections: i) in the low temperature region (< 300°C), two sharp endothermic peaks appear in the derivative DSC at about 120-130 (more intense) and 230-240°C. The former, causing

a 9% weight loss, can be attributed to the departure of both superficially adsorbed and loosely bound zeolitic H<sub>2</sub>O; the latter, causing a further 4% weight loss, to the removal of residual H<sub>2</sub>O and the first fraction of structural OH<sub>2</sub>. ii) in the central region (300-600°C), a broad endothermic peak at 520-530°C can be related to release of residual OH<sub>2</sub>, causing a further 5% weight loss. iii) in the high temperature region (> 600°C) a narrow endothermic peak followed by a broader exothermic maximum can be observed at 920 and 950-980°C respectively, the former being related to dehydroxilation and irreversible folding of the clay structure – a process reputed to start at lower temperatures (550°C)<sup>62</sup> – and the latter to possible phase transformation to clinoenstatite<sup>63</sup> or an amorphous phase.<sup>62</sup> These occurrences cause no further decrease in weight. The global weight loss is approximately 18%.

(INSERT FIGURE 5)

Loss of OH<sub>2</sub> merits further discussion: though previous studies<sup>64</sup> proved that no correspondence exists between experimentally calculated H<sub>2</sub>O percentages and those derived from the theoretical model,<sup>65</sup> Mg-coordinated OH<sub>2</sub> is expected to be lost over a wide temperature range, i.e. to start immediately after the release of the last fraction of zeolitic H<sub>2</sub>O (210-220°C) and to be complete before dehydroxilation. Recent diffraction studies,<sup>66</sup> consistent with previous TGA,<sup>67</sup> proved that loss of OH<sub>2</sub> occurs in two steps: the first half is lost between 202 and 267°C and the residual between 307 and 452°C. In spite of the renowned difficulties in sharply attributing weight percentages inferred from TGA to zeolitic H<sub>2</sub>O or structural OH<sub>2</sub>,<sup>60</sup> it is assumed that most of the 230-240°C and the 520-530°C endothermic maxima can be related to the loss of the 1<sup>st</sup> and 2<sup>nd</sup> half of Mg-coordinated OH<sub>2</sub> respectively.

TGA/DSC data collected for pristine methyl-red in air (not shown) are consistent with previous studies.<sup>40</sup> No weight loss occurs below 200°C, though a small exothermic transition attributed to *trans*- to *cis*-isomerization can be appreciated at 180°C. A

drastic weight loss (25%) is registered between 200 and 230°C, accompanied by an endothermic maximum (230°C) associated to molecule combustion. Weight loss proceeds gradually with temperature rise until complete consumption.

Adsorption of methyl red on palygorskite causes significant changes in both the TGA and derivative DSC patterns (Fig. 6). Most important variations are: i) two endothermic peaks, analogous to those described for pure palygorskite, appear in the derivative DSC below 300°C, but the global weight loss is reduced with respect to the pristine clay (11 vs. 13%, respectively). ii) a never-before seen, sharp endothermic peak appears in the DSC at 390-400°C. As no analogous band is observed for the pure clay, this feature is expected to be related to loss and combustion of the guest methyl red dye. Reliability of this attribution is supported by the corresponding weight loss (measured in the 300-400°C interval) being approximately 2%, well matching with the dye amount purposely added to the clay during synthesis of the hybrid pigment. At higher temperature (500°C), a weaker endothermic peak can be related to release of the residual structural OH<sub>2</sub> fraction, whose departure is likely to start between 250-260°C (shoulder in DSC); the related weight loss (4%) is lower than that occurring in pure palygorskite (5%). iii) no significant change affects the region above 600°C.

(INSERT FIGURE 6)

In order to evaluate the effects of heating on the colour and optical properties of the studied hybrid material, diffuse reflectance UV-vis data were collected in different steps of the adopted temperature ramp. The related patterns are shown in Figure 7.a. Heating causes both absorption maxima in the visible range (540 and 580 nm respectively) to progressively decrease in intensity until complete disappearance: such a behavior is consistent with gradual deterioration of the methyl red molecules adsorbed on palygorskite. The intensity decay with heating is slightly more effective on the 580 nm band (Figure 7.b), basically showing for both maxima a linear decrease



which causes them to almost zero at  $T > 350^{\circ}\text{C}$  (Figure 7.b). Further heating (up to  $450^{\circ}\text{C}$ ) flattens all visible bands, causing the related spectrum (Fig. 7.a) to be similar to that of pristine palygorskite.

UV-vis spectra collected using the same temperature ramp on pristine methyl red specimens (not shown), though following a more complicated trend, basically show that absorption bands in the visible range tend to disappear below  $300^{\circ}\text{C}$  consistently with the above commented TGA results.

(INSERT FIGURE 7)

#### 4. Discussion

All experimental evidences suggest that in the studied hybrid material supramolecular host/guest interactions form between the hosting palygorskite matrix and the guest dye, which is in agreement with previous results<sup>36</sup> and literature studies on analogous methyl red-intercalated adducts.<sup>40</sup>

Because of its reactivity, the methyl red carboxyl group is likely to be mostly involved in interacting with the hosting clay, a fact already hinted by previous UV-vis data (decay of the 290 nm maximum – see figure 4 in Giustetto and Wahyudi, 2011).<sup>36,68</sup> Though the correspondent IR spectral region is superposed to the more intense palygorskite  $\nu(\text{Si-O})$  bands, involvement of the dye  $-\text{C}=\text{O}$  group as an H-bond acceptor could be ascertained.<sup>25,48,56,58,69</sup>

Existence of H-bonds, known to be responsible for the unusual stability of analogous palygorskite and/or sepiolite-based adducts with indigo,<sup>25,33,41,50,70</sup> is further confirmed by the detected perturbations which involve a small Mg-coordinated  $\text{OH}_2$  fraction, presumably acting as H-bond donor for the methyl red carbonyl.<sup>25,41,50</sup> These interactions can form inside the palygorskite tunnels and/or in the grooves (half-channels) furrowing the fibres surface,<sup>19</sup> supporting the assumption of an intervened incorporation of methyl red inside the clay pores.

The collected spectroscopic outcomes give also specific information about the configuration of the incorporated dye molecules. Before sorption, pure methyl red is mostly in its neutral *trans*-form<sup>71,72</sup> though presence of a subordinate *cis*- isomer cannot be completely excluded;<sup>73,74</sup> transformation of one form to another can be switched by pH fluctuations or exposure to electromagnetic wavelengths.<sup>75</sup> Encapsulation inside the palygorskite pores triggers, at least in part, transformation of methyl red *trans*-form [Fig. 8, (a)] to its possible quinoid zwitterionic intermediates, namely an intramolecular H-bonded tautomer<sup>56</sup> and a non-bonded one [Fig. 8, (b) and (c) respectively].<sup>36,76,77</sup> Such transformations, possibly favoured by contextual presence of the strong donor-acceptor couple of dimethylamino and carboxyl groups,<sup>71</sup> reduce  $\pi$ -electron density on the central azoic bond due to conversion from a double (N=N) to a single bond (N–N)<sup>51</sup> and tend to stabilize after completion of the hybrid pigment synthesis. These zwitterionic azo derivatives possibly contribute to formation and tightening of host/guest interactions due to presence of strong donor-acceptor groups on both precursors,<sup>66,67,71, 76,77</sup> which may justify existence of Coulombic attractive forces.

(INSERT FIGURE 8)

Gradual transformation of one zwitterionic tautomer (non-intramolecular hydrogen bonded form) to another (intramolecular H-bonded form) is likely to characterize the different steps of the clay/dye complex formation.<sup>67,71</sup> Such an evolution, catalyzed by heating and Soxhlet treatments, may also suggest appearance of a third, additional quinoid zwitterion with temperature rise which may form an inter-molecularly hydrogen bonded complex with the hosting framework, a hypothesis already hinted in literature.<sup>71</sup> Contextual presence in the hybrid material of several zwitterionic tautomers is consistent with the sorption of methyl red on an electrostatic unbalanced hosting matrix such as palygorskite.

In addition to zwitterions, the clay-adsorbed methyl red molecules may also appear in the form of modified *trans*-isomers perturbed by gradual formation and strengthening of interactions with the clay framework.

It appears therefore that several kinds of different bonding types may exist between the clay and the dye – each contributing to the exceptional stability of this hybrid material, which rivals that of Maya Blue itself. The proposed analogy is well-grounded as also stability of this Pre-Columbian pigment is guaranteed by similar effects related to various kinds of interactions<sup>24</sup> co-existing in different sites<sup>31</sup> – i.e. inside the host microtunnels or in the superficial grooves.<sup>19</sup> No significant loss of structural OH<sub>2</sub> nor structural folding is likely to happen by heating (150°C) a previously activated/evacuated palygorskite + methyl red (2 wt%) ground mixture. Such a behavior is opposed to that of pristine palygorskite, whose heating in vacuum at 150°C causes almost 50% OH<sub>2</sub> loss and folding of the clay structure.<sup>54,55,57</sup> Presence of methyl red in the tunnels of palygorskite apparently prevents structural folding while affecting release of structural OH<sub>2</sub> 1<sup>st</sup> half, a situation analogous to that observed in sepiolite, a similar microporous clay, for which incorporation of indigo under equivalent *T* and vacuum conditions implies non-folding of the clay structure.<sup>5,50</sup> Phase transition due to appearance of di-hydrated palygorskite (expected at  $\cong 252^\circ\text{C}$  in air<sup>71</sup> and 150° in vacuum<sup>55,57</sup> for the pristine clay) is therefore unlikely to happen in the heated hybrid pigment. Partial structural disorder caused by limited structure folding, however (i.e. methyl red-free tunnel portions or located near the fibre edges, with or without OH<sub>2</sub> loss),<sup>55</sup> cannot be completely excluded.

Basic invariance of the evacuated hybrid material spectral features before and after heating [Fig. 2, part (b), curves 1 and 2 respectively] implies that formation of host/guest interactions is likely to be complete already after grinding, assuming that palygorskite is preliminarily activated before adding the dye. Such a treatment, in fact, is expected to cause zeolitic H<sub>2</sub>O loss while preserving the whole structural OH<sub>2</sub> amount. Departure of zeolitic H<sub>2</sub>O achieved through palygorskite activation or heating is a fundamental step to allow bonding to the dye. Such an assumption further supports the fact that methyl red fixation involves diffusion inside the clay tunnels or grooves rather than merely sticking on the fibre surface.

The role of heating is therefore of less importance when a pre-activated clay/dye ground mixture is concerned, as such a step just ensures strengthening of host/guest interactions already established during grinding consequent to clay activation and zeolitic H<sub>2</sub>O loss.

Conversely, heating becomes a fundamental step to allow formation of mutual bonds when the hybrid pigment is prepared in air at room temperature, for mere grinding *per se* is not effective to cause zeolitic H<sub>2</sub>O loss, achievable only by heating the mixture. Such a treatment, when applied in average environmental conditions, triggers perturbations in the dye molecule configuration causing spectroscopic data collected on merely ground or heated specimens to substantially differ.<sup>36</sup>

To further support the abovementioned assumptions, UV-vis diffuse reflectance data were collected on pre-activated palygorskite mixed and ground under N<sub>2</sub> atmosphere with 2 wt% methyl red (Fig. 9, curve 1, dot-dashed) prior to heating. This pattern is quite different from that related to an analogous unheated clay/dye adduct ground in average environmental conditions (curve 2 in Fig. 9, taken from Giustetto and Wahyudi).<sup>36</sup> As pre-activation of palygorskite causes loss of most zeolitic H<sub>2</sub>O to occur without heating, the ground mixture (curve 1 in Fig. 9) shows both an absorption decrease of the 465 nm band (*trans*-isomer perturbation, due to formation of mutual bonds) and a weak red-shift (from 560 to 566 nm) of the zwitterions maximum, thus implying that host/guest interactions are already established at this stage. It is noteworthy to remark that for these spectral features to become manifest when the hybrid pigment is synthesized in average environmental conditions, further heating and Soxhlet extraction are necessary.<sup>36</sup> Such a trend confirms that crushing of pre-activated palygorskite in N<sub>2</sub> with a 2 wt% methyl red is more than sufficient to ensure adequate stabilization of the dye in the clay matrix, even without heating.

(INSERT FIGURE 9)

Further rehydration and Soxhlet extraction in ethanol removes any non-bonded dye surplus (isolated or crystalline methyl red *trans*-isomer) from the pigment, leaving the bound *trans*-

form and zwitterions unaffected and possibly strengthening their links to the hosting matrix (shift towards higher wavelengths of the 540 and 580 nm UV-vis maxima: see fig. 4 in Giustetto and Wahyudi, 2011).<sup>36,40</sup>

Persistence of the adsorbed dye as zwitterions or perturbed *trans*-isomers in the clay framework is hard to destabilize, as previously performed stability tests to chemical agents and pH fluctuations proved. Only treatment with HCl apparently affects the clay-incorporated dye, somehow modifying its bonding to the host and causing an appreciable chromatic variation (from purplish to red).<sup>36</sup> Further stability checks proved that neither prolonged solar/UV-A irradiation nor thermal treatment trigger appreciable transformations in the encapsulated dye molecules, as no shift affects the related spectral maxima. All treatments, however, cause progressive degradation thus explaining the consequent bleaching of the hybrid pigment hue. Though sharp identification of molecular species from absorption spectra is tricky,<sup>78</sup> consistently with the attributions suggested by literature<sup>36,71-74,79</sup> the methyl red zwitterions are less severely affected by sunlight exposure with respect to the perturbed *trans*-isomer form, whose maximum (540 nm) undergoes a more significant decay. An opposite trend is observed by severely heating the hybrid material, for it is the zwitterions maximum (580 nm, main contributor to the pigment colour) to suffer a more severe intensity decrease. *Trans*- to *cis*-isomerisation, sometimes catalyzed by specific irradiation,<sup>75</sup> is not likely to occur. Colour fading due to progressive dye degradation proceeds linearly with time. Sorption of methyl red in palygorskite, however, causes such bleaching to be significantly slower with respect to that observed for pure methyl red exposed to analogous conditions. The palygorskite framework plays therefore a fundamental role in sheltering the guest molecules, which is consistent with their intervened incorporation in the host micropores. When progressively heated, the red/purplish colour of the hybrid material is maintained, though progressively reduced in intensity, until  $T = 350^{\circ}\text{C}$ ; a further  $50^{\circ}\text{C}$  increment causes the specimen to almost completely bleach ( $400^{\circ}\text{C}$ : Fig. 7.a). Such a behavior is consistent with the endothermic

degradation of the clay-adsorbed dye and is further confirmed by the related weight loss corresponding to that of the added methyl red amount (almost 2%).

Stability of methyl red to both irradiation with specific wavelengths and thermal treatment is therefore markedly enhanced by incorporation and bonding in the hosting palygorskite microtunnels. The mutual clay/dye interaction significantly affects the thermal features of the resulting hybrid material with respect to its isolated precursors. Sorption of methyl red in palygorskite causes a lower quantity of weakly-bound H<sub>2</sub>O to leave the hosting framework during dehydration. Such reduction, possibly related to zeolitic H<sub>2</sub>O, implies that in the synthesized pigment part of the channels volume is occupied by the incorporated guest molecules. Sheltering guaranteed by intervened encapsulation causes the adsorbed dye to apparently decompose at significantly higher temperatures (390-400°C) with respect to its pure, isolated counterpart (200°C), a trend already observed on similar methyl red intercalated hybrid materials.<sup>40</sup>

## 5. Conclusions

A stable red/purple hybrid pigment can be obtained by mixing, grinding and heating (140°C for several hours) palygorskite with 2 wt% methyl red. Such a complex possesses the same stability of Maya Blue as neither its color nor its structure are significantly affected by chemical attacks.<sup>36</sup> While fixation on other microporous materials (i.e. zeolites) preserves methyl red activity to pH fluctuations and related color changes allowing production of solid phase indicators,<sup>39</sup> sorption on palygorskite shields and stabilizes the azo-dye, whose color does not sensibly change in spite of drastic pH variations, and keep it *in situ* thanks to supramolecular host/guest interactions. Use of palygorskite instead of sepiolite ensures the adopted hosting framework to be stronger and

more stable,<sup>80,81</sup> although the reduced size of the pores (maximum width: 6.4 vs. 10.6 Å respectively) inevitably limits the possibility of incorporating bigger guest molecules. Feasible diffusion of methyl red inside the palygorskite micropores was already hinted in literature<sup>36</sup> thanks to the dimensional compatibility between the tunnels maximum effective width (6.4 Å) and the molecule minimum steric impediment (6.0 Å). This hypothesis is corroborated by the fundamental role played by heating or evacuation during the hybrid pigment synthesis, processes which are responsible for clay activation, zeolitic H<sub>2</sub>O loss and dye incorporation inside the emptied tunnels or superficial grooves (Fig. 10).

(INSERT FIGURE 10)

Methyl red encapsulation affects the structural features of the hosting matrix preventing folding with heating (150°C in vacuum, due to concrete unfeasibility for the dye-occupied tunnels to collapse) and modifying its tendency to retain structural OH<sub>2</sub>. The same phenomenon modifies the thermo-optical features of the azo dye, enhancing its stability and colour resistance.

Different kinds of host/guest interaction (H-bonding and electrostatic attractive forces) coexist and contribute to the exceptional stability of the studied hybrid material, a situation apparently occurring as well in the analogous clay/indigo Maya Blue adducts.<sup>31</sup> It cannot be excluded, however, that further interactions might develop according to the magnitude of heating applied during synthesis. Straight bonds could form between the dye carboxyl group and the peripheral TOT Mg ions, once the 1<sup>st</sup> OH<sub>2</sub> half is removed due to temperature rise. These bonds, described for analogous hybrid materials subjected to severe thermal treatments,<sup>5,22</sup> are known to lack stability favouring gradual reverse to OH<sub>2</sub>-mediated H-bonds consequent to relentless rehydration of palygorskite cooled in a hydrating environment.<sup>32</sup>

As in Maya Blue, where indigo loses its planarity<sup>21,47</sup> due to partial oxidation to dehydroindigo,<sup>23,82-84</sup> sorption of methyl red in its multiple configurations (modified trans-isomer and zwitterions) might involve slight distortions of the molecule thus facilitating diffusion inside the palygorskite microtunnels.

## Acknowledgements

The authors would like to thank Prof. Giacomo Chiari of the Getty Conservation Institute, Los Angeles (U.S.A.), who first thought Mayan pigments could be other than blue.

We thank Serena Corallini and Marco Travet for their precious help in collecting UV-vis and TGA data respectively, and Francesca Bonino for her obstinate but vain attempts in trying to obtain acceptable Raman spectra.

The authors would also like to thank the reviewers of this paper (anonymous), who helped with their ideas, hints and suggestions to significantly improve the quality of the manuscript.

Special thanks go to Prof. Giovanni Ferraris, who helped supporting this research.

## References

- [1] E. Ruiz-Hitzky, *J. Mater. Chem.* 11 (2001) 86-91.
- [2] G. Calzaferri, S. Huber, H. Maas, C. Minkowski, *Angewandte Chemie* 42 (2003) 3732-3758.
- [3] R. Fernandez-Saavedra, P. Aranda, R. Ruiz-Hitzky, *Adv. Funct. Mater.* 14 (2004) 77-82.
- [4] C. Sanchez, B. Julià, P. Belleville, M. Popall, *J. Mater. Chem.* 15 (2005) 3559-3592.
- [5] F. Ovarlez, S. Giulieri\*, A.M. Chaze, F. Delamare, J. Raya, J. Hirschinger, *Chem. Eur. J.* 15(2009) 11326-11332.
- [6] D. Brühwiler, G. Calzaferri, T. Torres,; J.H. Ramm, N. Gartmann, L.Q. Dieu, I. Lòpez-Duarte, M.V. Martínez-Díaz, *J. Mater. Chem.* 19 (2009) 8040-8067.
- [7] L. Dong Feng, B. Qing Chen, Y. Ying Shi, Y. Wei Guo, J. Huang, M. Sun, Y. Xin Gu, D. Hao, *Advanced Materials Research* 78 (2011) 8-16.
- [8] C. Yue, L. Hongwei, Z. Fei, C. Hukui, R. Xiaoning, L. Ziqiang, *Chemical Engineering Journal* 167(1) (2011) 183-189.
- [9] K. Hu, K. Zheng, X. Tian, L. Chen, L. Sun, X. Shui, *Journal of Macromolecular Science B – Physics* 50,5 (2011) 846-859.
- [10] T. Chen, H. Liu, J. Li, D. Chen, D. Chang, D. Kong, R.L. Frost, *Chemical Engineering Journal* 166(3) (2011) 1017-1021.



- [11] C. Reyes-Valerio, De Bonampak al Templo Mayor: el Azul Maya en Mesoamerica, Ed. Siglo XXI, Mexico, 1993.
- [12] H. Van Olphen, *Science* 154 (1966) 645-646.
- [13] R. Kleber, L. Masschelein-Kleiner, J. Thissen, *Studies in Conservation* 12 (1967) 41-55.
- [14] S. Guggenheim, R.A. Eggleton, *Reviews in Mineralogy* 19 (1988) 675-725.
- [15] R. Giustetto, G. Chiari, *Eur. Journ. of Mineral.* 16 (2004) 521-532.
- [16] S.W. Bailey, A. Alietti, G.W. Brindley, M.L.L. Formosa, K. Jasmund, J. Konta, R.C. Mackenzie, K. Nagasawa, R.A. Rausell-Colom, B.B. Zvyagin, *Clays and Clay Minerals* 28 (1980) 73-78.
- [17] E. Garcia-Romero, M. Suarez Barrios, M.A. Bustillo Revuelta, *Clays and Clay Minerals* 52 (2004) 486-494.
- [18] M. Suarez, E. Garcia-Romero, *Applied Clay Science* 31 (2006) 154-163.
- [19] G. Chiari, R. Giustetto, J. Druzik, E. Dohene, G. Ricchiardi, *Applied Physics A* 90 (2008) 3-7.
- [20] G. Chiari, R. Giustetto, G. Ricchiardi, *Eur. Journ. of Mineral.* 15 (2003) 21-33.
- [21] R. Giustetto, D. Levy, G. Chiari, *Eur. Journ. of Mineral.* 18 (2006) 629-640.
- [22] S. Ovarlez, A.M. Chaze, F. Giulieri, F. Delamare, *Comptes Rendu Chimie* 9 (2006) 1243-1248.
- [23] L.A. Polette-Niewold, F.S. Manciu, B. Torres, M. Alvarado Jr, R.R. Chianelli, *Journ. Of Inorganic Biochemistry* 101 (2007) 1958-1973.
- [24] A. Doménech, M.T. Doménech-Carbò, M. Sánchez del Río, M.L. Vázquez de Agredos Pascual, *Journal of Solid State Electrochemistry* 13 (2009) 869-878.
- [25] R. Giustetto, F. Llabres I Xamena, G. Ricchiardi, S. Bordiga, A. Damin, M. Chierotti, R. Gobetto, *J. Phys. Chem. B* 109(41) (2005) 19360-19368.
- [26] E. Fois, A. Gamba, A. Tilocca, *Microporous and Mesoporous Materials* 57 (2003) 263-272.
- [27] D.Reinen, P.Köhl, C. Muller, *Zeitschrift für anorganische und allgemeine Chemie* 630 (2004) 97-103.
- [28] F.S. Manciu, A. Ramirez, W. Durrer, J. Govani, R.R. Chianelli, *Journal Of Raman Spectroscopy* 39 (2008) 1257-1261.
- [29] A. Tilocca, E. Fois, *J. Phys. Chem. C* 113 (2009) 8683-8687.
- [30] M.E.Fuentes, B.Peña, C.Contreras, A.L.Montero, R.Chianelli, M.Alvarado, R.Olivas, L.M.Rodriguez, H.Camacho, L.A. Montero-Cabrera, *Int. Journ. of Quantum Chem.* 108(10) (2008) 1664-1673.
- [31] A. Doménech, M.T. Doménech-Carbò, M. Sanchez del Rio, M.L. Vazquez de Agredos Pascual, E. Lima, *New Journal of Chemistry* 33 (2009) 2371-2379.
- [32] S. Ovarlez, F. Giulieri, F. Delamare, N. Sbirrazzuoli, A.M. Chaze, *Microporous and Mesoporous Materials* 142 (2011) 371-380.
- [33] M. Sanchez Del Rio, E. Boccaleri, M.Milanesio, G. Croce, W. Van Beek, C. Tsiantos, G.D. Chryssikos, V. Gionis, G.H. Kacandes, M. Suarez, E. Garcia-Romero, *J. Mater. Sci.* 44 (2009) 5524-5536.
- [34] Y. Ozdemir, M. Dogan, M. Alkan, *Microporous and Mesoporous Materials* 96 (2006) 419-427.
- [35] M. Dogan, Y. Ozdemir, M. Alkan, *Dyes and Pigments* 75 (2007) 701-713.
- [36] R. Giustetto, O. Wahyudi, *Microporous and Mesoporous Materials* 142 (2011) 221-235.

- [37] R.J. Gettens, *American Antiquity* 27 (1962) 557-564.
- [38] G. Simha Martynková, L. Kulhanková, P. Maly, P. Capková, *Journal of Nanoscience and Nanotechnology* 8(4) (2008) 2069-2074.
- [39] K. Huddersman, V. Patruno, G.J. Blake, R.H. Dahm, *Coloration Technology JSDC* 114 (1998) 155-159.
- [40] Y. Tian, G. Wang, F. Li, D.G. Evans, *Materials Letters* 61 (2007) 1662-1666.
- [41] R. Giustetto, K. Seenivasan, S. Bordiga, *Periodico di Mineralogia* 79 (2010) 21-37.
- [42] J.R. Durig, W.M. Zunic, T.G. Costner, G.A. Guirgis, *Journal of Raman Spectroscopy* 24(5) (2005) 281-285.
- [43] A. Bisset, T.J. Dines, *J. Chem. Soc. Faraday Trans.* 91(3) (1995) 499-505.
- [44] S. Bell, A. Bisset, T.J. Dines, *Journal of Raman Spectroscopy* 29 (1998) 447-462.
- [45] P. Sun-Kyung, L. Choongkeun, M. Kyung-Chul, L. Nam-Soo, *Bull. Korean Chem. Soc.* 25 (2004) 1817-1821.
- [46] L. Szetsen, W. Jian-How, L. Shiao-Jun, *Appl. Spectroscopy* 65(9) (2011) 996-1003.
- [47] K. Witke, K.W. Brzezinka, I. Lamprecht, *Journal of Molecular Structure* 661-662 (2003) 235-238.
- [48] D.A. McKeown, J.E. Post, E.S. Etz, *Clays and Clay Minerals* 50(5) (2002) 667-680.
- [49] M. Sánchez del Río, M. Picquart, E. Haro-Poniatowski, E. Van Elslande, V. Hugo Uc, *Journal of Raman Spectroscopy* 37 (2006) 1046-1053.
- [50] R. Giustetto, K. Seenivasan, F. Bonino, G. Ricchiardi, S. Bordiga, M.R. Chierotti, R. Gobetto, *J. Phys. Chem. C* 115(34) (2011) 16764-16776.
- [51] N. Biswas, S. Umaphathy, *J. Phys. Chem. A* 104 (2000) 2734-2745.
- [52] A. Blisset, T.J. Dines, *J. Chem. Soc. Faraday Trans.* 91(3) (1995) 499-505.
- [53] R. Prost, Ph.D. Thesis (1975) University of Paris VI.
- [54] C.J. Serna, G.E. Van Scoyoc, J.L. Ahlrichs, *Amer. Miner.* 62 (1977) 784-792.
- [55] G.E. Van Scoyoc, C.J. Serna, J.L. Ahlrichs, *Amer. Miner.* 64 (1979) 215-223.
- [56] H. Hayashi, R. Otsuka, N. Imai, *Amer. Miner.* 53 (1969) 1613-1624.
- [57] C. Blanco, J. Herrero, S. Mendioroz, A. Pajares, *Clays and Clay Minerals* 36(4) (1988) 364-368.
- [58] R.L. Frost, O.B. Locos, H. Ruan, J.T. Kloprogge, *Vibrational Spectroscopy* 27 (2001) 1-13.
- [59] J.L. Martin Vivaldi, P. Fenoll Hach-Ali, in: R.M. Mackenzie (Ed.), *Differential thermal analysis*, Academic Press, London, 1970, pp. 553-573.
- [60] B.F. Jones, E. Galan, in: S.W. Bailey (Ed.), *Hydrous phyllosilicates*, *Reviews in Mineralogy* 19, Mineralogical Society of America, Washington, 1988, pp. 631-674.
- [61] G. Artioli, E. Galli, E. Burattini, G. Cappuccio, S. Simeoni, *N. Jb. Miner. Mh.* 5 (1994) 217-229.
- [62] J.E. Post, P.J. Heaney, *Amer. Miner.* 93 (2008) 667-675.
- [63] A. Preisinger, *Clays and Clay Minerals* 10 (1963) 365-371.

- [64] A. Mifsud, M. Rautureau, V. Fornes, *Clays and Clay Minerals* 13 (1978) 367-374.
- [65] W.F. Bradley, *Amer. Miner.* 25 (1940) 405-410.
- [66] N. Yasarawan, J.S. Van Duijneveldt, *Langmuir* 24 (2008) 7184-7192.
- [67] G. Gabor, Y. Frey, D. Gegiou, M. Kaganowitch, E. Fischer, *Israel Journal Chemistry* 5 (1967) 193-212.
- [68] K.M. Tawarah, S.J. Khouri, *Dyes and Pigments* 20 (1992) 261-270.
- [69] S. Aisawa, S. Takahashi, W. Ogasawara, Y. Umetsu, E. Narita, *J. Solid State Chem.* 162 (2001) 52-62.
- [70] R. Giustetto, D. Levy, O. Wahyudi, G. Ricchiardi, J.G. Vitillo, *Eur. Journ. of Mineral.* 23 (2011) 449-466.
- [71] S. Mukherjee, S. Chandra Bera, *J. Chem. Soc., Faraday Trans.* 94(1) (1968) 67- 71.
- [72] D. Fedorenko, E. Ouskova, V. Reshetnyak, Y. Reznikov, *Physical Review* (2006) DOI: 10.1103/PhysRevE.73.031701.
- [73] W.R. Brode, J.H. Gould, G.M. Wyman, *J. Am. Chem. Soc.* 74 (1952) 4641-4646.
- [74] J. Bieth, S.M. Vratsanos, N.H. Nasserman, A.G. Coopers, B.F. Erlanger, *Biochemistry* 12 (1973) 3023-3027.
- [75] M. Ogawa, K. Kuroda, *Chem. Rev.* 95 (1995) 399-438.
- [76] P.D. Wildes, J.C. Pacifici, G. Irick Jr, D.G. Whitten, *J. Am. Chem. Soc.* 93 (1971) 2004.
- [77] N. Nishimura, S. Kosako, Y. Sueishi, *Bull. Chem. Soc. Jpn.* 67 (1984) 1617-1625.
- [78] W.C. Ross, G.P. Warwick, *J. Chem. Soc.* (1956), 1719-1724.
- [79] E. Fischer, Y. Frei *J. Chem. Phys.* 27 (1957) 328-330, DOI:10.1063/1.1743709.
- [80] M. Sanchez Del Rìo, P. Martinetto, C. Reyes-Valerio, E. Dooryhée, M. Suárez, *Archaeometry* 48(1) (2006) 115-130.
- [81] R. Giustetto, O. Wahyudi, I. Corazzari, F. Turci, *Appl. Clay Science* 52 (2011) 41-50.
- [82] A. Doménech, M.T. Doménech-Carbò, M.L. Vàsquez de Agredos Pascual, *J. Phys. Chem. B* 110 (2006) 6027-6039.
- [83] A. Doménech, M.T. Doménech-Carbò, M.L. Vàsquez de Agredos Pascual, *J. Phys. Chem. C* 111 (2007) 4585-4595.
- [84] R. Rondão, J.S. Seixas de Melo, V.D.B. Bonifácio, M.J. Melo, *J. Phys. Chem. A* 114 (2010) 1699-1708.

## Figure captions

- Fig. 1. The structure of monoclinic palygorskite<sup>15</sup>; unit cell is marked by continuous lines and z-elongated microchannels are deprived of zeolitic H<sub>2</sub>O for sake of clarity (a); Acid red 2 (C<sub>15</sub>H<sub>15</sub>N<sub>3</sub>O<sub>2</sub>, C.I. 13020 – methyl red) dye molecule (b).
- Fig. 2. Part a): FTIR spectra of pristine methyl red as solid-state powder diluted in KBr (grey curve) and in benzene solution (solvent contribution subtracted; black curve). Part b): FTIR spectra of pre-activated (in vacuum at 150°C) palygorskite + methyl red (2 wt%) mixed and ground under N<sub>2</sub> atmosphere (1), heated in vacuum at 150°C (2) and after re-hydration in air and Soxhlet extraction in ethanol (3). Inset c) magnification of the  $\delta(\text{OH})$  band of the pre-activated mixed and ground hybrid material, evidencing a shoulder at 1632 cm<sup>-1</sup>.
- Fig. 3. Effect of prolonged solar-like irradiation (100 hours) on the diffuse reflectance UV-visible spectra of the palygorskite + methyl red (2 wt%) adduct (a); intensity decrease of the absorption maxima in the visible range (540 and 580 nm) (b).
- Fig. 4. Effect of prolonged UV-A irradiation (76 hours) on the diffuse reflectance UV-visible spectra of the palygorskite + methyl red (2 wt%) adduct (a); intensity decrease of the 580 nm absorption maximum (b).
- Fig. 5. Observed TGA (a) and DSC (b) curves for palygorskite in air in the 0-1000°C temperature range.
- Fig. 6. Observed TGA (a) and DSC (b) curves for the palygorskite + methyl red (2 wt%) adduct in air in the 0-1000°C temperature range.
- Fig. 7. Effect of progressive heating [room temperature (RT) to 450°C] on the diffuse reflectance UV-visible spectra of the palygorskite + methyl red (2 wt%) adduct (a); intensity decrease of the absorption maxima in the visible range (540 and 580 nm) (b).
- Fig. 8. The acid red 2 (methyl red) molecule in *trans*-form (a), intra-molecular hydrogen bonded quinoid zwitterion (b) and non-bonded quinoid zwitterion (c).<sup>51</sup>
- Fig. 9. Diffuse reflectance UV-Visible spectrum of a pre-activated (120°C in N<sub>2</sub>) and evacuated (pressure below 5x10<sup>-4</sup> mbar) palygorskite + methyl red (2 wt%) adduct mixed and ground under N<sub>2</sub> atmosphere (curve 1, grey and dashed) compared to that of a non-pretreated palygorskite + methyl red (2 wt%) adduct mixed and ground in average environmental conditions (in air at room temperature) (curve 2, black, taken from Giustetto and Wahyudi, 2011<sup>36</sup>). Spectra were obtained on powder samples diluted with BaSO<sub>4</sub> (1: 3 ratio).
- Fig. 10. Juxtaposition and encapsulation of methyl red molecule inside the palygorskite superficial grooves (a) and microtunnels (b and c) respectively. Specific H-bonds and electrostatic interactions form between the dye carboxyl group and the clay Mg-coordinated OH<sub>2</sub> (dashed lines), thus stabilizing the hybrid material. Notice how the limited amount of methyl red added to palygorskite (2 wt%) causes not all channels to be filled by the dye molecules. The residual channels are empty (while heating or in vacuum) or re-filled by weakly bound zeolitic H<sub>2</sub>O (in average environmental conditions; not shown for sake of clarity).

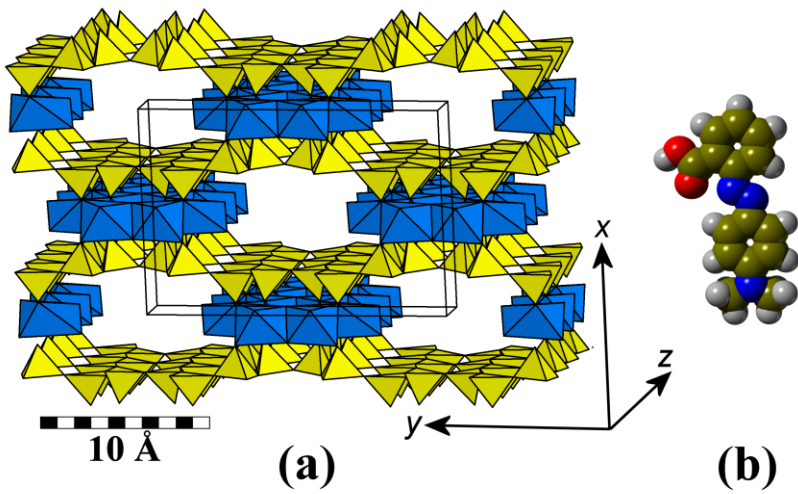


Figure 1

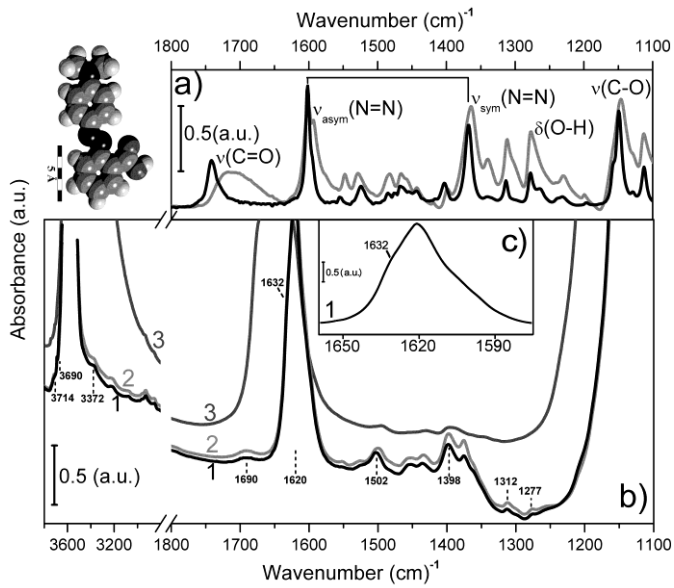


Figure 2

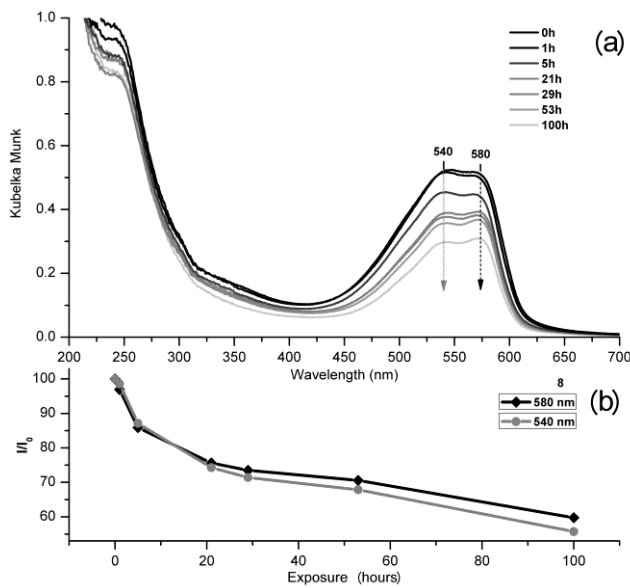


Figure 3

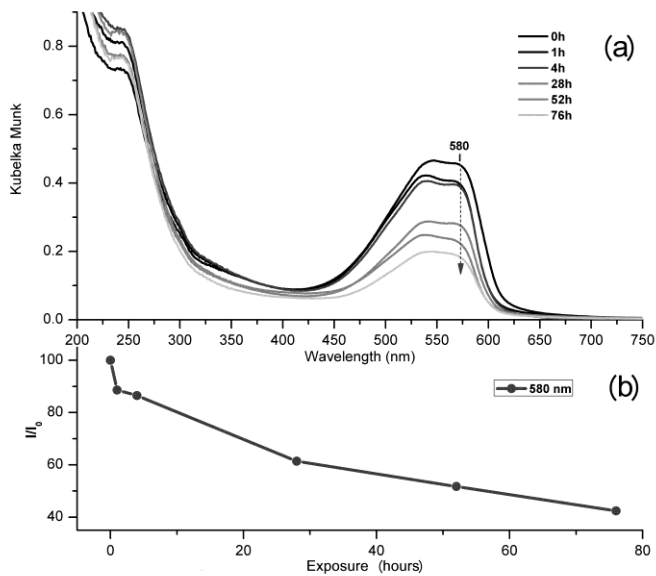


Figure 4

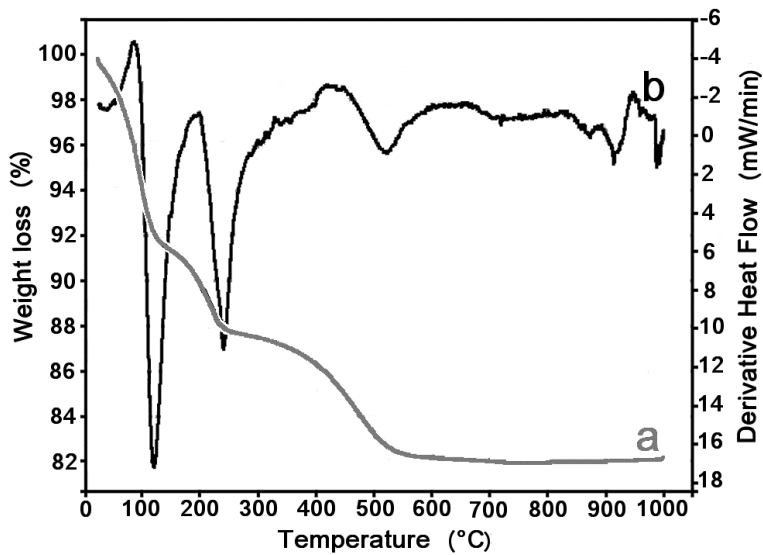


Figure 5

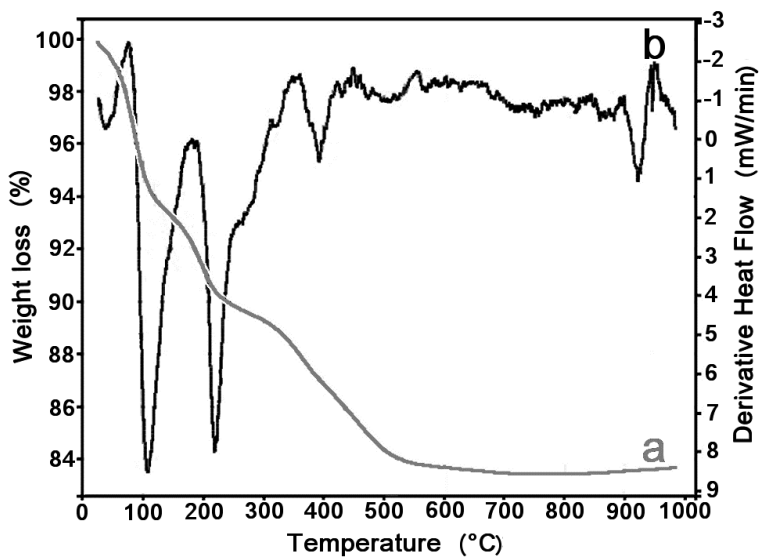


Figure 6

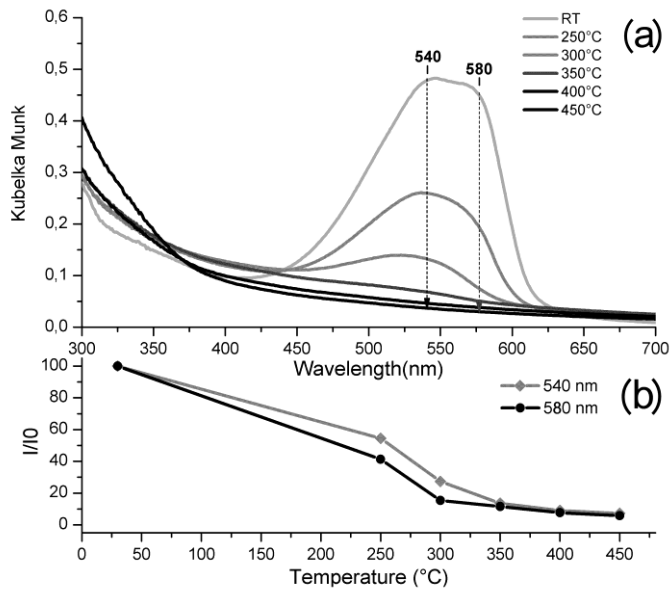


Figure 7

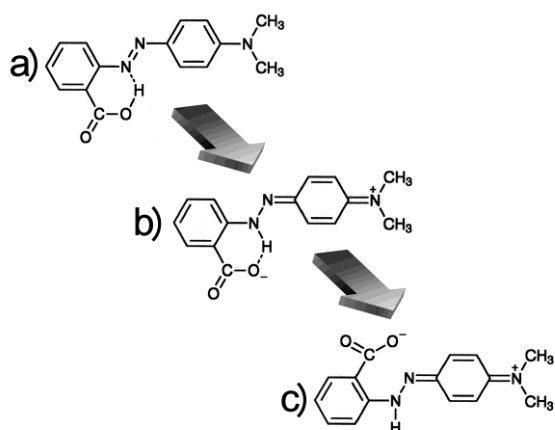


Figure 8

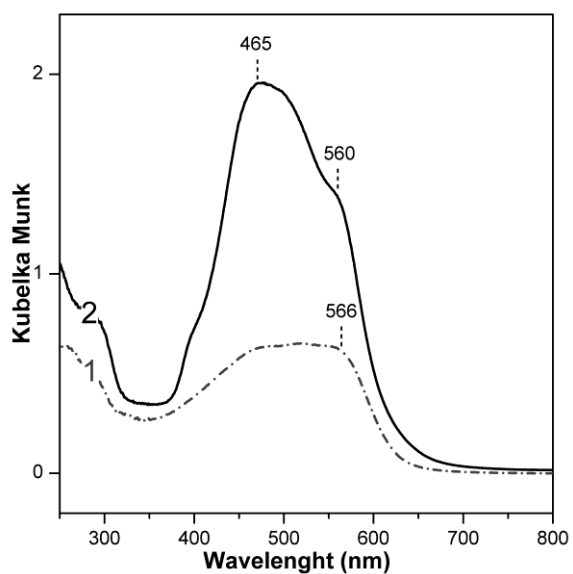


Figure 9

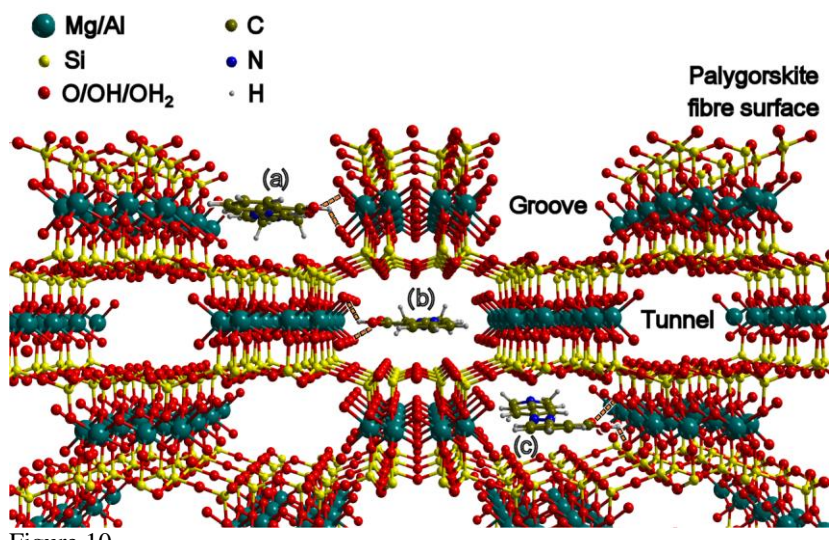


Figure 10